

Semester Thesis

Force Sensing Catheter

Florian Berlinger

George Chatzipirpiridis

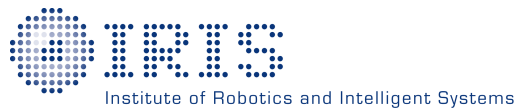
Adviser

Prof. Dr. Bradley J. Nelson

Institute of Robotics and Intelligent Systems

Swiss Federal Institute of Technology Zurich (ETH)

February 2015





Eidgenössische Technische Hochschule Zürich
Swiss Federal Institute of Technology Zurich

Declaration of originality

The signed declaration of originality is a component of every semester paper, Bachelor's thesis, Master's thesis and any other degree paper undertaken during the course of studies, including the respective electronic versions.

Lecturers may also require a declaration of originality for other written papers compiled for their courses.

I hereby confirm that I am the sole author of the written work here enclosed and that I have compiled it in my own words. Parts excepted are corrections of form and content by the supervisor.

Title of work (in block letters):

Force Sensing Catheter

Authored by (in block letters):

For papers written by groups the names of all authors are required.

Name(s):

Berlinger

First name(s):

Florian

With my signature I confirm that

- I have committed none of the forms of plagiarism described in the '[Citation etiquette](#)' information sheet.
- I have documented all methods, data and processes truthfully.
- I have not manipulated any data.
- I have mentioned all persons who were significant facilitators of the work.

I am aware that the work may be screened electronically for plagiarism.

Place, date

Zurich, 22/02/2015

Signature(s)

For papers written by groups the names of all authors are required. Their signatures collectively guarantee the entire content of the written paper.

Preface

This semester thesis was written at the Institute of Robotics and Intelligent Systems (IRIS), which is part of the Swiss Federal Institute of Technology Zurich (ETH), during the fall term 2014. The impulse to do so was my general interest in the field of robotics in combination with my desire to contribute to a real-world medical application.

First, I would like to express my gratitude to my supervisors, George Chatzipirpiridis and Dr. Olgaç Ergeneman, for their support and advice during my research.

Thanks as well to Prof. Dr. Bradley J. Nelson, head of the Multi-Scale Robotics Lab (MSRL) at ETH, for giving me the opportunity to write my semester thesis there.

Additionally, I would like to thank Alex Greber from ALTATEC, a highly specialised Swiss company in microelectronics, for his collaboration regarding the wiring of the Hall sensor.

Moreover, I very much appreciate the love, enthusiasm and moral encouragement, which friends and family have shown to me.

Finally, thank you Simone Gervasoni. I was lucky to find your expertise during your internship at the MSRL. Besides, I very much appreciated our discussions on all kind of crazy inventions. It was a pleasure to meet you.

Abstract

The Force Sensing Catheter is able to sense axial and lateral contact forces at its distal end. A flexible membrane connects an axially aligned Hall sensor with a permanent magnet. The membrane is squeezed whenever an external force acts on the catheter head.

The need for the Force Sensing Catheter arises from a medical fact: The success of cardiac ablations for the treatment of arrhythmia highly depends on the applied contact force from the catheter tip to the body tissue.

The first series of prototypes of the Force Sensing Catheter is manufactured on a 3D-printer. Outer diameters of 3.5 mm and less allow for easy navigation inside the human blood vessels.

The newly designed Force Sensing Catheter offers three advantages over the state of the art, namely catheters using optical fibres or strain gauges. Firstly, it comes with a simple and compact design and is capable to measure contact forces with the help of a highly affordable Hall sensor. Secondly, it supports navigation through external magnetic fields using the built-in permanent magnet. Thirdly, the current catheter localisation through X-rays may become obsolete by tracking the permanent magnet.

Key words: Magnetic catheter, Contact force (CF), MEMS, Microsystems, Biomedical devices, Cardiac ablation

Zusammenfassung

Der Force Sensing Catheter misst axiale und laterale Kontaktkräfte an der Katheterspitze. Eine flexible Membran verbindet einen axial zentrierten Hall-Sensor mit einem Permanentmagneten. Die Membran wird zusammengepresst, sobald eine externe Kraft auf den Katheterkopf wirkt.

Das Bedürfnis nach dem Force Sensing Catheter beruht auf einer medizinischen Tatsache: Der Erfolg von kardialen Ablationen zur Behandlung von Herzrhythmusstörungen hängt stark von der Kontaktkraft ab, die von der Katheterspitze auf das Körpergewebe wirkt.

Die ersten Prototypen des Force Sensing Catheters werden mit einem 3D-Drucker hergestellt. Aussendurchmesser von 3.5 mm und weniger erlauben die problemlose Fortbewegung innerhalb der menschlichen Blutgefäße.

Der neu entwickelte Force Sensing Catheter weist drei Vorteile auf gegenüber dem Stand der Technik, nämlich Kathetern, die optische Fasern oder Dehnmessstreifen verwenden. Erstens kommt er im einfachen und kompakten Design daher und misst Kontaktkräfte mit Hilfe eines günstigen Hall-Sensors. Zweitens erlaubt das eingebaute Permanentmagnet die Steuerung durch externe Magnetfelder. Drittens erübriggt sich die Lokalisierung des Katheters mit Röntgenbildern dank der möglichen Verfolgung der Magnetposition.

Schlagworte: Magnetischer Katheter, Kontaktkraft, MEMS, Mikrosysteme, Biomedizinische Geräte, Kardiale Ablation

Contents

Preface	iii
Abstract	v
Zusammenfassung	vii
List of Tables	xi
List of Figures	xiii
Notation	xv
1 Introduction	1
1.1 State of the art in contact force sensing catheters	2
1.2 Contributions towards contact force sensing catheters	2
1.3 Structure of this thesis	3
2 Force Sensing Catheter designs	5
2.1 Force sensing principle	5
2.2 3D Force Sensing Catheter	6
2.3 1D Force Sensing Catheter	11
2.4 Comparison between the Force Sensing Catheter models	13
3 Experiments with the Force Sensing Catheter	15
3.1 Experimental set-up and test scenarios	15
3.2 Theory-based hypotheses	16
3.3 Catheter calibration	16
3.4 Catheter validation	19
3.5 Material stiffness assessment	20
3.6 Tissue diagnosis	21
4 Conclusion	23
4.1 Limitations of the Force Sensing Catheter	23
4.2 Outlook for future improvements	24
4.3 Possible applications of the Force Sensing Catheter	24

4.4	Advantages of the Force Sensing Catheter	25
	References	27
A	Functional principle of a Hall sensor	29
B	Simulations for the membrane deflection	31
C	Code for the experiments	35
C.1	Trajectory generation	35
C.2	Data post-processing	37

List of Tables

1	Comparison between the specifications of the 3D and the 1D Force Sensing Catheter.	13
---	--	----

List of Figures

1	Radiofrequency ablation for the treatment of arrhythmia[2]: A contact force sensing catheter isolating defective tissue inside the human heart.	1
2	State-of-the-art contact force sensing catheters: TactiCath™ Quartz[7] (left) and Thermocool® SmartTouch®[1] (right).	2
3	Contact force overview[7]: A contact force sensing catheter measuring axial and lateral forces at its distal end.	3
4	Force sensing principle: A flexible membrane that squeezes under contact forces connects a permanent magnet with a Hall sensor. . .	6
5	Configuration of the 3D Force Sensing Catheter: a) assembly, b) Hall sensor at the catheter tip, c) complete catheter, d) catheter inside a human heart chamber (model).	7
6	Excerpt from the data sheet of the magnet used for experiments[4] (left) and the corresponding simulation for the red Hall sensor operation range (right).	8
7	Sandwich structure of the membrane: stiff plugs in grey and flexible crushing zone in black.	10
8	Elements of the 1D Force Sensing Catheter: a) assembled catheter, b) magnet, membrane, Hall sensor on PCB, mounted PCB, catheter tube (LTR), c) membrane mold.	11
9	Configuration of the 1D Force Sensing Catheter: a) wired Hall sensor on a flexible PCB, b) assembly, c) Hall sensor on a finger tip. .	12
10	Experimental set-up consisting of a balance, a micro-manipulator and the Hall sensor inside the catheter head.	15
11	Axial calibration test run: fully released (a) to fully squeezed (d).	17
12	Axial magnetic field - displacement behaviour: simulated (left) and experimental (right).	17
13	Axial displacement - force behaviour.	18
14	Lateral calibration test run: fully released (a) and fully squeezed (b).	19
15	Lateral displacement - force behaviour (left) and magnetic field - force behaviour (right).	19

16	Catheter validation: measured force values versus calculated force values.	20
17	Assessment of different material stiffnesses: steeper force - displacement curves for stiffer materials.	21
18	Force Sensing Catheter pushing muscle tissue.	21
19	Tissue flexibility mapping.	22
20	Functional principle of a Hall sensor.	29
21	Deflection of a radially fixed silicon disk under a contact force.	31
22	Membrane deflections in dependency of the applied force for different thicknesses.	32
23	Membrane deflection: hand validation of the COMSOL simulations.	32
24	Membrane deflection of the 1D Force Sensing Catheter.	33

Notation

Symbols

F	contact force [mN]
k	membrane stiffness [N/mm]
d	membrane displacement [mm]
B	B-field [T]
m	magnetic flux density (sensor value) [mG]
I	current [A]
U	voltage [V]

Indices

x	x-direction
y	y-direction
z	z-direction

Acronyms and Abbreviations

FSC	Force Sensing Catheter
ETH	Eidgenössische Technische Hochschule
IRIS	Institute of Robotics and Intelligent Systems
MSRL	Multi-Scale Robotics Lab
PCB	Printed circuit board

1 Introduction

The key feature of the Force Sensing Catheter is its ability to measure applied contact forces of the catheter head on body tissue. The need for such contact force information arises from medical treatments and diagnoses using catheters.

A major application of force sensing catheters is the radiofrequency ablation for the treatment of cardiac arrhythmia, visualised in Figure 1. Arrhythmia is caused by electrical heartbeat impulses which either take abnormal routes along the heart tissue or which are sent out by other heart cells than the responsible sinus node. The defective tissue is destroyed by applying radiofrequency energy at a certain contact force. Monitoring this contact force helps doctors applying the correct pressure during ablation treatments. Staying within a certain pressure range during the ablation procedure is crucial as shown in [6] and [11]. Too high pressure possibly leads to complications like steam pops whereas too low pressure does not cause the desired healing effect.

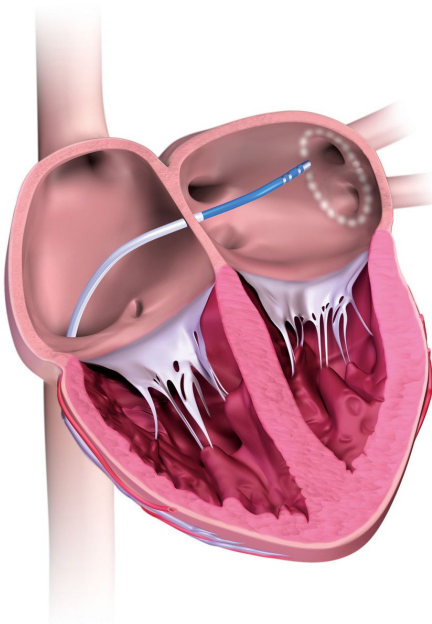


Figure 1: Radiofrequency ablation for the treatment of arrhythmia[2]: A contact force sensing catheter isolating defective tissue inside the human heart.

This thesis includes the design and the experimental validation of a realistically dimensioned catheter that is able to measure contact forces.

1.1 State of the art in contact force sensing catheters

A variety of technologies to measure contact forces exists. However, only two principles have been successfully implemented into medical catheters so far. On the one hand, St.Jude Medical's TactiCathTM Quartz uses optical fibers to detect the forces acting on the catheter head. On the other hand, Thermocool® SmartTouch® of Biosense Webster makes use of a strain gauge¹.



Figure 2: State-of-the-art contact force sensing catheters: TactiCathTM Quartz[7] (left) and Thermocool® SmartTouch®[1] (right).

Both catheters, the TactiCathTM Quartz and the Thermocool® SmartTouch®, have an outer diameter of 3.5 mm. They are able to measure axial and lateral contact forces. Navigation/steering is done by hand while mapping happens through X-rays.

1.2 Contributions towards contact force sensing catheters

The main goal of this thesis is to prove a novel force sensing principle consisting of a Hall sensor and a permanent magnet within a realistically dimensioned catheter design. Two prototypes are developed in order to validate the new force sensing

¹TactiCathTM Quartz and Thermocool® SmartTouch® are discussed in [9]. More information is available online on their respective websites [1], [7].

idea. The 3D version is capable to measure axial and lateral forces (see Figure 3). It has an outer diameter of 3.5 mm. The 1D model measures axial forces only but comes with a smaller outer diameter of 1.6 mm.

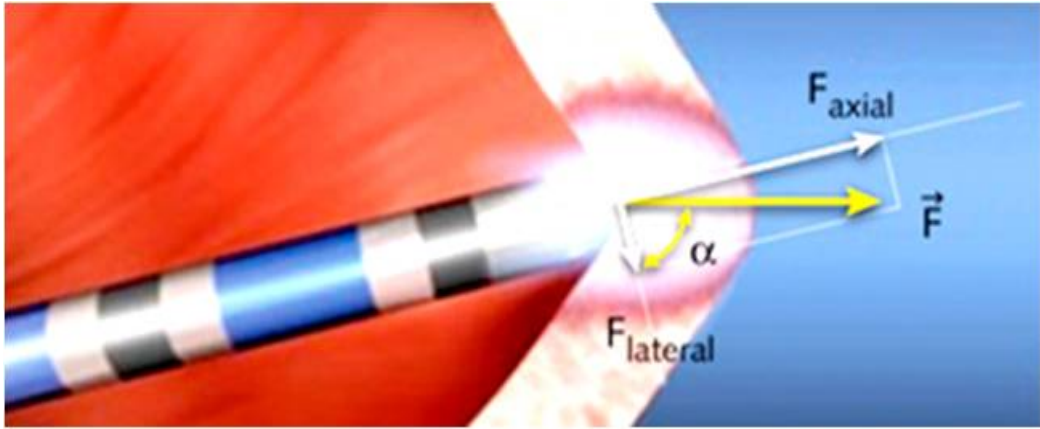


Figure 3: Contact force overview[7]: A contact force sensing catheter measuring axial and lateral forces at its distal end.

The Force Sensing Catheter makes three major contributions towards the state of the art. Firstly, it simplifies the force measurement principle by using a Hall sensor in combination with a permanent magnet. This new approach for the 3D contact force measurement will probably allow a significant reduction of the current catheter diameters.

Secondly, the design of the Force Sensing Catheter that includes a strong permanent magnet allows the navigation/steering of the catheter head with external magnetic fields, e.g. by using an electromagnetic system like the OctoMag[5].

Finally, mapping through X-rays may become obsolete. The built-in permanent magnet is locatable using the same electromagnetic system that steers the catheter head.

1.3 Structure of this thesis

This thesis is split into two main parts.

Chapter 2 briefly explains the force sensing principle consisting of a Hall sensor and a permanent magnet. Subsequently, it describes the design of the 3D and the 1D Force Sensing Catheter.

Chapter 3 focuses on the experiments. It describes the experimental set-up, states theory-based hypotheses and discusses their validation with the experimental findings.

Finally the conclusion summarises the thesis. It shows the limits of the present Force Sensing Catheter as well as recommendations for future developments.

For interested readers, the appendix offers additional and more detailed background insight into the working principle of Hall sensors, simulations for the membrane behaviour and programs for the evaluation of measurement data.

2 Force Sensing Catheter designs

The Force Sensing Catheter is developed for medical treatments and diagnoses inside the human body. This operating environment sets some limiting design constraints including dimensions and biocompatibility. Most importantly, the catheter diameter has to be as small as possible in order to allow for maximal mobility inside blood vessels. Miniature dimensions strongly influence the available manufacturing options and clearly limit the possible complexity of the device.

Two different designs of the Force Sensing Catheter were developed. The 3D model with an outer diameter of 3.5 mm measures axial and lateral forces. The smaller 1D model is capable to measure axial forces and has an outer diameter of 1.6 mm. Both models work with a Hall sensor and a permanent magnet. However, they are manufactured and assembled differently.

A brief explanation of the force sensing principle is followed by the illustration of the 3D and the 1D Force Sensing Catheter models.

2.1 Force sensing principle

The force sensing principle consists of a Hall sensor which is flexibly connected to a permanent magnet as shown in Figure 4. The permanent magnet emits a B-field which is measured by the Hall sensor². The measured B-field varies with the distance between the magnet and the Hall sensor. A flexible membrane that is placed between the magnet and the sensor allows a change of their relative positions. This positional change is caused by an applied contact force. A relation between the measured B-field and the contact force can be found by performing a sensor calibration with a balance and a micro-manipulator (see Chapter 3.3).

²The functional principle of a Hall sensor is explained in Appendix A.

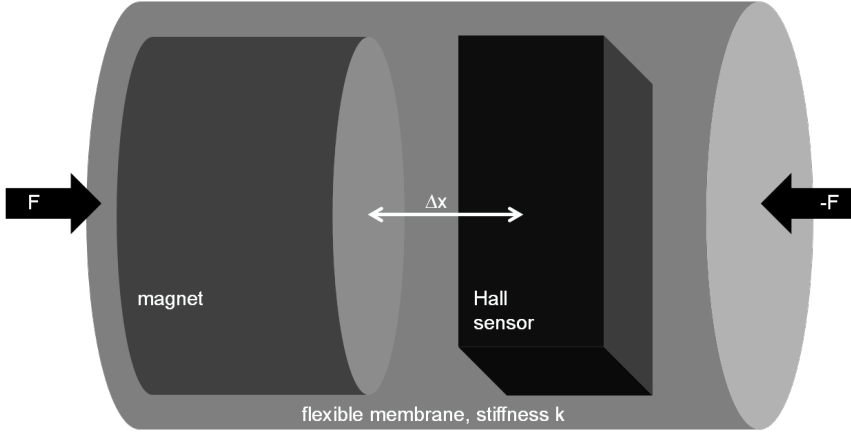


Figure 4: Force sensing principle: A flexible membrane that squeezes under contact forces connects a permanent magnet with a Hall sensor.

2.2 3D Force Sensing Catheter

The 3D model of the Force Sensing Catheter is able to measure contact forces in all three dimensions, i.e. axial and lateral forces. It is manufactured on an Objet500 Connex3 3D printer from Stratasys[10].

The basic design of the 3D Force Sensing Catheter is shown in Figure 5. The stiff parts called head and magnet holder host the Hall sensor[8] and the permanent ring magnet[4] respectively. The flexible membrane is mounted in between. The catheter tube is an off-the-shelf part that is readily available on the medical market.

All the parts are connected through glued plugs in order to ensure a proper axis alignment and an easy assembly procedure as shown in picture a) of Figure 5. The wires run through the middle of the catheter along its axis.

The outer diameter of the 3D catheter equalises the state-of-the-art of 3.5 mm (cf. Chapter 1.1). On the one hand, it is limited by the printer resolution of roughly $100 \mu\text{m}$. Simple geometries are feasible only. The minimum wall thickness for cylindrical shapes is around $200 \mu\text{m}$. On the other hand, the built-in Hall sensor comes with a quadratic surface of 2 mm by 2 mm. Thus, its diagonal length is $2 \text{ mm} \cdot \sqrt{2} = 2.82 \text{ mm}$. Consequently, diameters below 3 mm are unrealistic with the current Hall sensor (see Figure 5, b)). Picture d) in Figure 5 illustrates the current catheter dimensions by showing a prototype model inside a real-size human heart chamber.

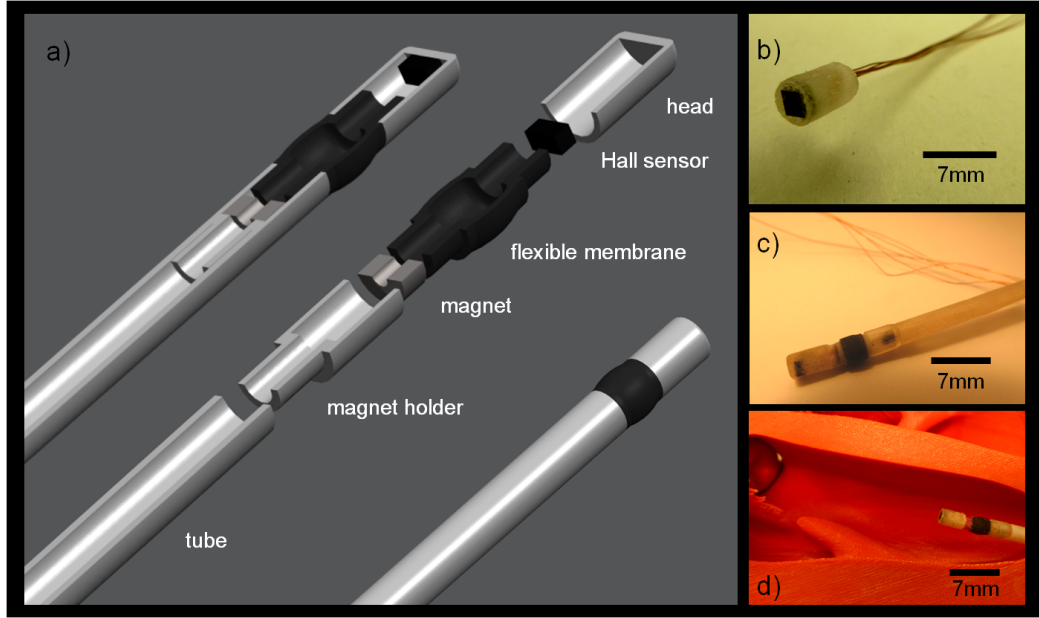


Figure 5: Configuration of the 3D Force Sensing Catheter: a) assembly, b) Hall sensor at the catheter tip, c) complete catheter, d) catheter inside a human heart chamber (model).

2.2.1 Wiring of the Hall sensor

The LIS3MDL Hall sensor from STMicroelectronics[8] is usually sold pre-wired on a spacious circuit board. In the case of the Force Sensing Catheter, a tailor-made solution had to be found in order to meet dimension and flexibility constraints. Flexible printed circuit boards (PCB's) were assessed as an alternative to stiff circuit boards. Even those are generally too big and especially too expensive. Obviously, no other solution was as small as connecting the wires directly to the 12 pins of the sensor. However, the direct wiring of the cables was assessed impossible by most companies in microelectronics. The wiring difficulties were finally overcome thanks to the expertise and the help of ALTATEC³: The cables were wired below a microscope, using an extra small soldering bolt.

2.2.2 Choice and placement of the permanent magnet

Special attention had to be paid on the choice and the placement of the permanent magnet. To begin with, the decision to fix the magnet and to keep the Hall sensor

³ALTATEC is a highly specialised Swiss company in microelectronics: www.altatec.ch.

moveable is based on navigation ideas. Therefore, the Hall sensor was placed in the catheter head. It moves whenever a contact force squeezes the flexible membrane. Following the navigation idea, the permanent magnet has to be very strong in order to allow for optimal steering.

However, the Hall sensor saturates at +/- 16 Gauss[8]. Consequently, the magnetic flux density of the permanent magnet which is measured by the Hall sensor shall never exceed +/- 16 Gauss. This specification sets a minimum distance between the magnet and the sensor or a maximum flux density of the magnet respectively. The critical point for saturation occurs at the distance at which the flexible membrane is maximally compressed.

The magnet and the Hall sensor are 10 mm apart in the 3D Force Sensing Catheter which is used for the following experiments in Chapter 3. The axial membrane deflection range is about 1.5 mm. These two placement decisions define the Hall sensor displacement range which is shown in Figure 6 (encircled in red on the magnet data sheet in the left picture, enlarged with the help of a simulation in the right picture).

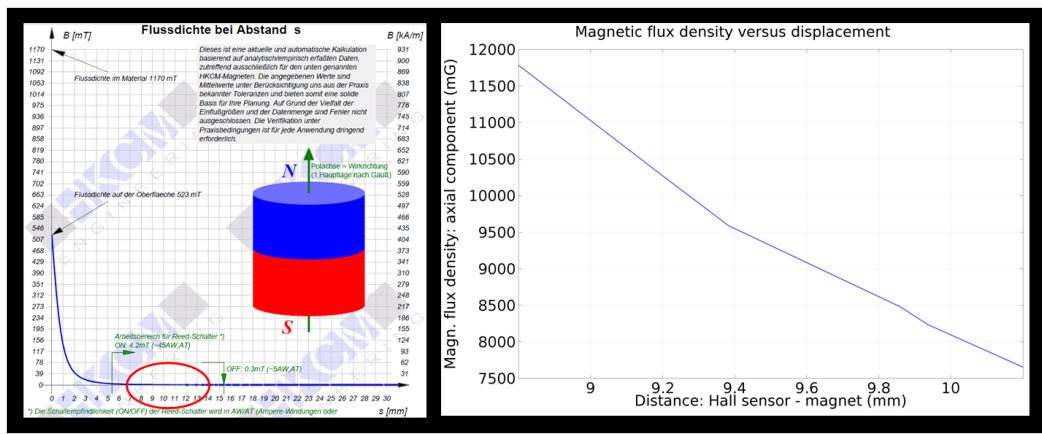


Figure 6: Excerpt from the data sheet of the magnet used for experiments[4] (left) and the corresponding simulation for the red Hall sensor operation range (right).

The B-field of a permanent magnet decays with the third potency of its distance from the magnet (Biot-Savart). Ideally, the magnet is used in its most significant B-field - distance range where the gradient of the decay-curve is the steepest (bottom left part of the left curve in Figure 6). This distance range would allow the most significant and, therefore, the most accurate B-field measurement

in dependence of the distance between the magnet and the Hall sensor.

All the above statements set constraints for the choice and the placement of the magnet. Furthermore, the stiffness of the flexible membrane and its deflection range are directly linked to the measurement accuracy of the B-field. A higher deflection range allows for larger changes in the measured magnetic flux densities.

The chosen magnet after simulations and tests is a 1.17 Tesla longitudinally magnetized ring magnet with the following dimensions: 3 mm outer diameter, 1.7 mm inner diameter and 0.5 mm height (cf. [4]: Magnet-Ring R03x01.7x00.5ND-N35). The ring shape allows to axially align the magnet with the catheter walls while guiding the wires through the centre of the magnet. The longitudinal magnetization favours axial B-field measurements.

2.2.3 Structure of the flexible membrane

There is a trade-off between a very strong magnet and its distance from the Hall sensor: the stronger the magnet, the bigger the distance has to be in order to avoid the saturation of the Hall sensor. There are three problems with big, i.e. long, membranes. First of all, they are hardly capable to transmit any lateral forces. Secondly, the catheter head as a whole loses its compactness. Thirdly, the magnet is not used in its optimal B-field - displacement range.

The membrane has to be designed in a way that its deflection allows for a significant enough change in B-fields. Moreover, the deflection shall be caused by reasonable contact forces⁴. Reasonable contact forces for radio-frequency cardiac ablations are around 20 g[11]. A significant enough change in B-fields can be found at around 1.5 mm axial membrane deflection or Hall sensor displacement respectively. The wall thickness of the membrane can be adjusted in order to reach the above force and deflection constraints. The current catheter comes with a membrane thickness of 0.5 mm.

The membrane is the only non-trivial catheter part to design. It is a composite of flexible and stiff 3D-printer materials. The two material types are attached to each other automatically during the printing process. The flexible crushing zone and the stiff plug connectors are interlaced in a sandwich structure. This membrane design enhances the deflection stability and durability.

⁴Simulations for the membrane behaviour at different thicknesses under a range of contact forces are presented in Appendix B.

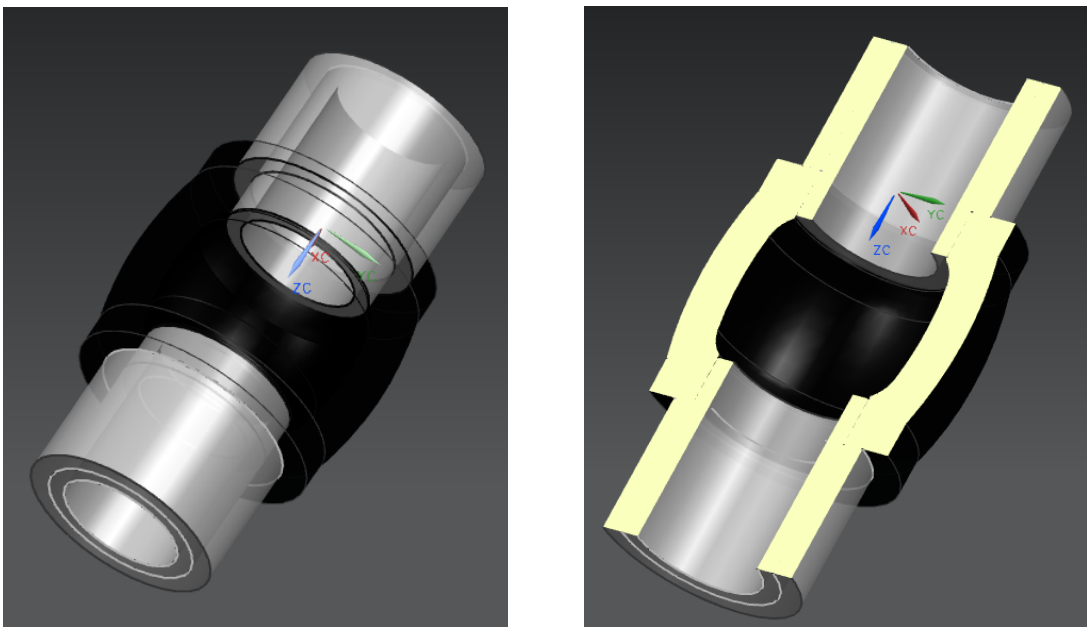


Figure 7: Sandwich structure of the membrane: stiff plugs in grey and flexible crushing zone in black.

The membrane shape is axially bulged in order to enhance straight axial deformations and to avoid uncontrolled buckling respectively. The main deflection direction is favourably along the long axis of the membrane.

2.3 1D Force Sensing Catheter

The general design concepts discussed so far hold for the 1D model of the Force Sensing Catheter as well. A smaller 1D Hall sensor is built-in the catheter head. This Hall sensor allows the measurement of axial forces. The outer diameter of the catheter is reduced to 1.6 mm.

The manufacturing process includes the 3D-printing of a mold, which is used to cast a silicon rubber membrane as shown in Figure 8.

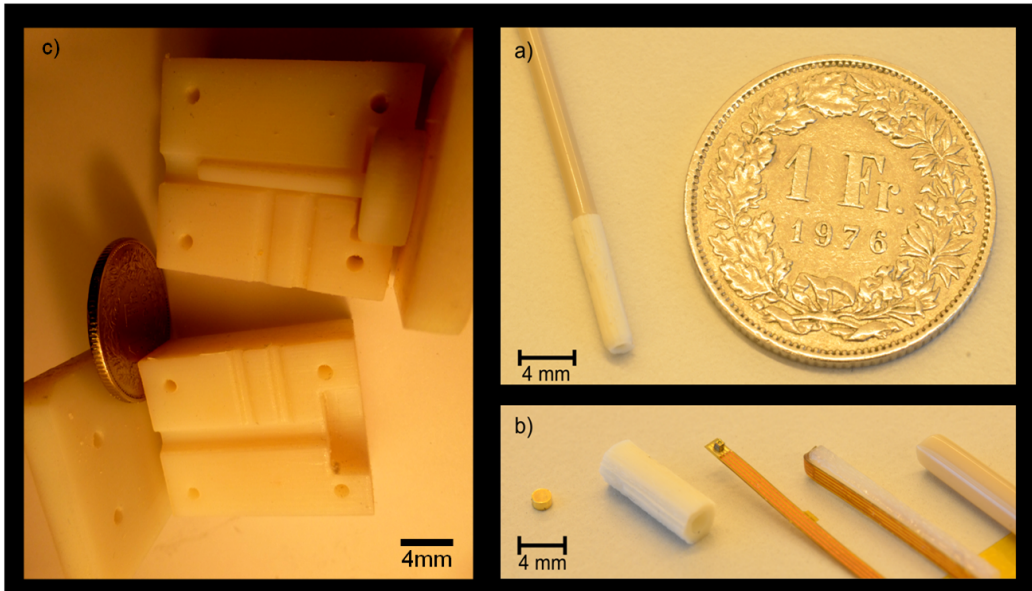


Figure 8: Elements of the 1D Force Sensing Catheter: a) assembled catheter, b) magnet, membrane, Hall sensor on PCB, mounted PCB, catheter tube (LTR), c) membrane mold.

The configuration of the 1D catheter slightly differs from the 3D one (see Figure 9). Most obviously, the magnet and the Hall sensor switch positions. The Hall sensor is now fixed to a 3D-printed sensor base. This sensor base is connected to the end of a biocompatible tube. The magnet sits at the top of the silicon rubber membrane. The squeezable silicon rubber membrane is finally put over the sensor base.

The decision to fix the Hall sensor at the sensor base and to place the magnet at the head is based on flexibility considerations. The membrane has to be able to move freely and equally in all directions. If the Hall sensor was placed at the

head, the connected PCB would run through the membrane and possibly disturb its free movement.

The wiring of the 1D Hall sensor is done on a flexible PCB provided by ALTATEC.

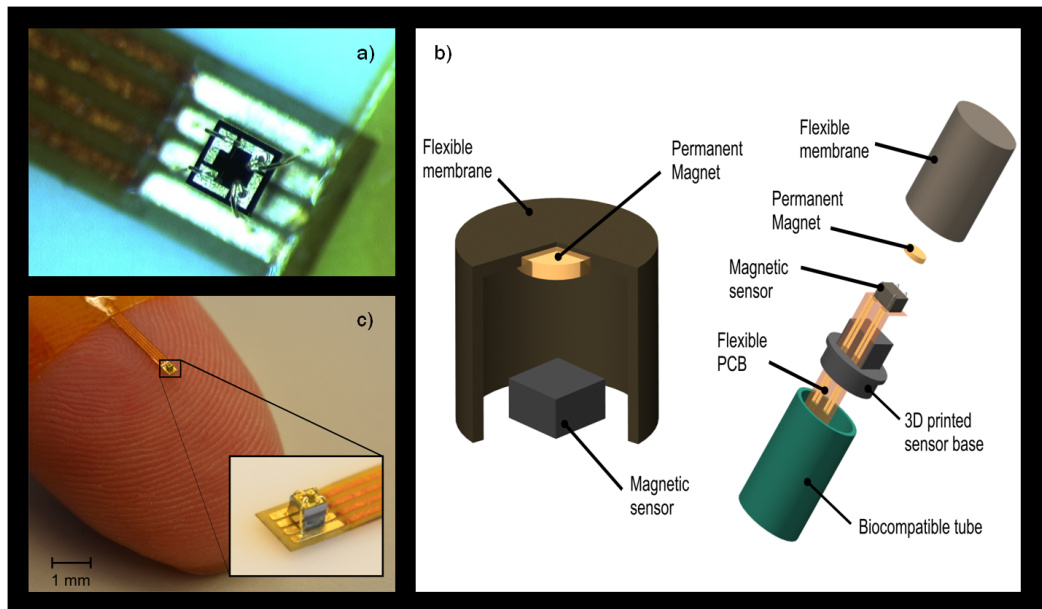


Figure 9: Configuration of the 1D Force Sensing Catheter: a) wired Hall sensor on a flexible PCB, b) assembly, c) Hall sensor on a finger tip.

2.4 Comparison between the Force Sensing Catheter models

A summary of the important features of the 3D and the 1D Force Sensing Catheters is shown in Table 1.

In brief, the 3D model is capable to measure axial and lateral forces but comes with a larger outer diameter than the simpler 1D model that measures axial forces only.

	3D catheter model	1D catheter model
Contact forces	Axial and lateral	Lateral
Outer diameter	3.5 mm	1.6 mm
Hall sensor position	Catheter head	Catheter base
Magnet position	Catheter base	Catheter head
Manufacture	3D-printed membrane and magnet/Hall sensor holders	Molded silicon membrane and 3D-printed base
Hall sensor wiring	Directly connected cables	Flexible PCB
Advantages	3D force measurements, magnetic steerability	Miniature outer diameter
Disadvantages	Complicated cable guidance	Expensive sensor wiring

Table 1: Comparison between the specifications of the 3D and the 1D Force Sensing Catheter.

3 Experiments with the Force Sensing Catheter

The experiments are intended to validate the novel force sensing principle consisting of a permanent magnet and a Hall sensor. All of the presented experimental data originate from test runs with the 3D catheter model.

This chapter discusses the experimental set-up, theory-based hypotheses and their respective experimental validation. Furthermore, advanced catheter applications are presented. One of these applications is capable to define material stiffnesses. The other application involves the development of a tissue diagnosis tool for the mapping of the tissue surface and the tissue flexibility.

3.1 Experimental set-up and test scenarios

The experimental set-up consists of three devices. They are shown in Figure 10. An OHAUS balance measures contact forces during the calibration procedure. A SmarAct micro-manipulator allows the precise steering of the catheter along three axes. The built-in Hall sensor delivers the measured magnetic flux density.

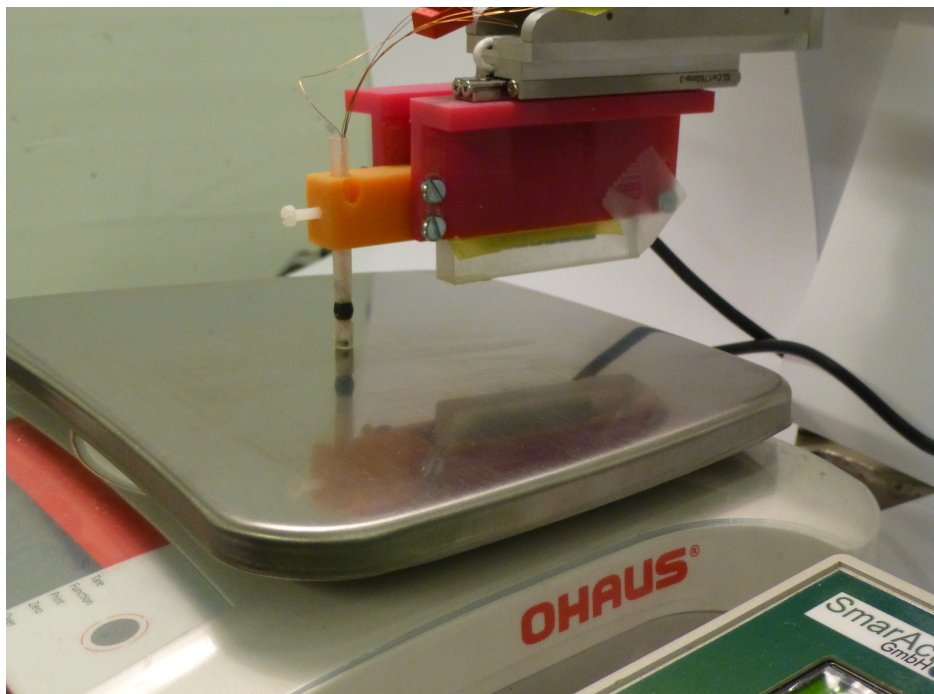


Figure 10: Experimental set-up consisting of a balance, a micro-manipulator and the Hall sensor inside the catheter head.

The three devices are connected to a computer operating LabView. A test run follows a pre-generated trajectory that is fed to the micro-manipulator. Measurement data from the Hall sensor and the balance as well as the effective trajectory are automatically recorded in a log-file. Data post-processing and visualisation happens in MATLAB⁵.

Every new catheter has to be calibrated before it is ready for usage. The goal of the calibration process is to find a relation between the measured magnetic flux density and the corresponding contact force.

3.2 Theory-based hypotheses

Beforehand it is to mention that the Force Sensing Catheter can be calibrated for any repeatable force - magnet field relation regardless of the theoretical expectations. A lookup table can be created as long as the force - magnetic field behaviour is consistent and repeatable.

Theory states two hypotheses for the Force Sensing Catheter. On the one hand, the force (F) - displacement (d) relation shall be linear according to Hooke's law (k can be considered to be the membrane stiffness): $F = -k \cdot d$. The linear force - displacement behaviour of the catheter membrane is verified through simulations in COMSOL. Analytical calculations can be executed according to "Roark's Formulas for Stress and Strain" [12], p.427-429, 455-459, 491-492.

On the other hand, the magnetic flux density decays with the third potency of the distance from the magnetic surface according to Biot-Savart. This behaviour is shown on the data sheet of the magnet in Figure 6. It is also simulated and verified with COMSOL. The analytical formulas for magnet fields emitted by permanent magnets are found in chapter 4 of "Permanent Magnet and Electromechanical Devices" [3] from Edward Furlani.

3.3 Catheter calibration

In a first step, the catheter is calibrated. To do so, the magnetic flux density is measured with the Hall sensor while the applied contact force is assessed with a balance. Subsequently, a relationship between the flux density and the force has

⁵Possible codes for the generation of trajectories and for the evaluation of the measurement data are shown in AppendixC.

to be found at every stage of the membrane deflection. The calibration process is executed twice: once for the axial forces (Figure 11) and once for the lateral forces (Figure 14). The right plot of Figure 12 illustrates the post-processed measurement points for the axial calibration. These measurement points are gained and averaged over 10 identical test runs. Each test run follows a vertical trajectory that pushes the catheter head on the balance. As a result, the membrane is deflected. A contact force as well as a change in the magnetic flux density can be measured.

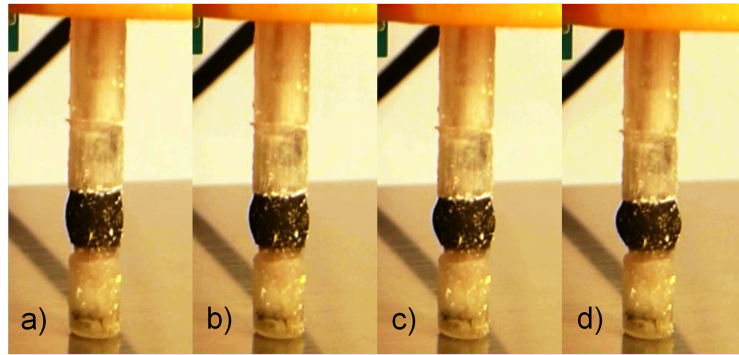


Figure 11: Axial calibration test run: fully released (a) to fully squeezed (d).

The left plot of Figure 12 shows the theoretical values that can be expected according to simulations (cf. Figure 6). Measurement data and theory agree well for the axial force case. Slight deviations may occur due to assembly inaccuracies. Radial or angular offsets of the magnet alignment against the Hall sensor and against the catheter axis respectively result in shifted B-field measurements.

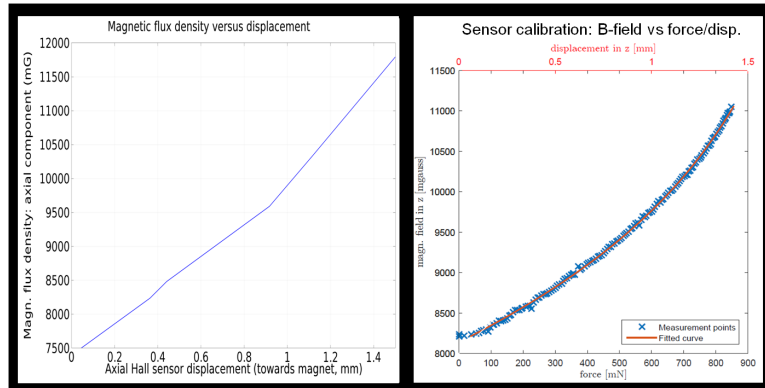


Figure 12: Axial magnetic field - displacement behaviour: simulated (left) and experimental (right).

The displacement - force relation is shown in Figure 13. The fact that it can be considered sufficiently linear allows to substitute the force axis in Figure 12 with the corresponding displacement axis.

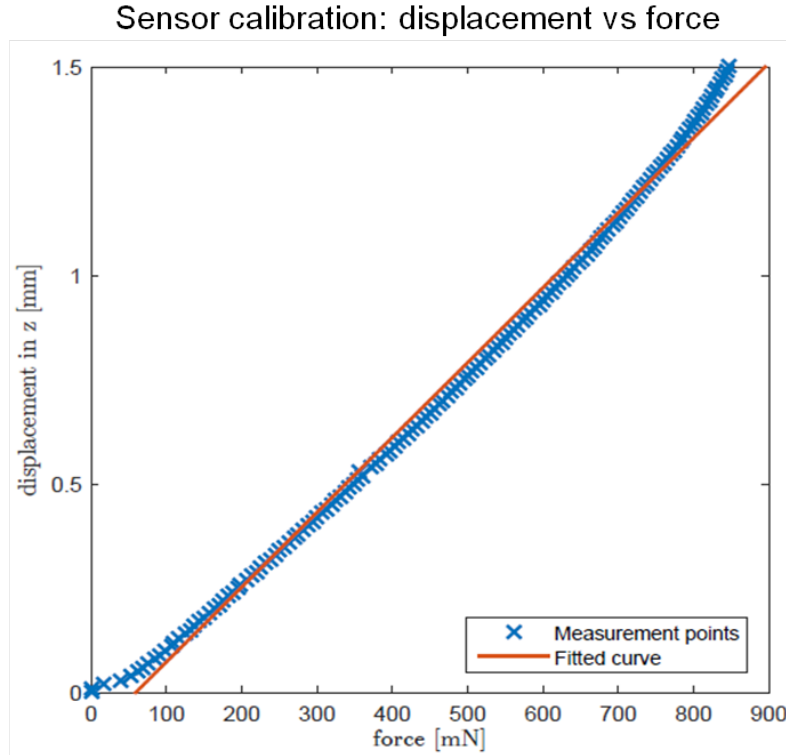


Figure 13: Axial displacement - force behaviour.

Finally, a linear regression with all the measurement points is done in MATLAB. The result is a fitted curve and its respective polynomial function. The measured magnetic flux density can be fed in the function; the applied contact force is passed back.

The same procedure can be done for the lateral force calibration (see Figures 14 and 15).

The calibration is successful as well. The experiments repeatedly show the same magnetic flux density - force behaviour. However, two obvious changes against the axial calibration case can be observed. Firstly, the displacement - force behaviour and the magnetic field - force behaviour do not match theoretical expectations any more. Secondly, the measurement range of the magnetic field shrinks drastically.

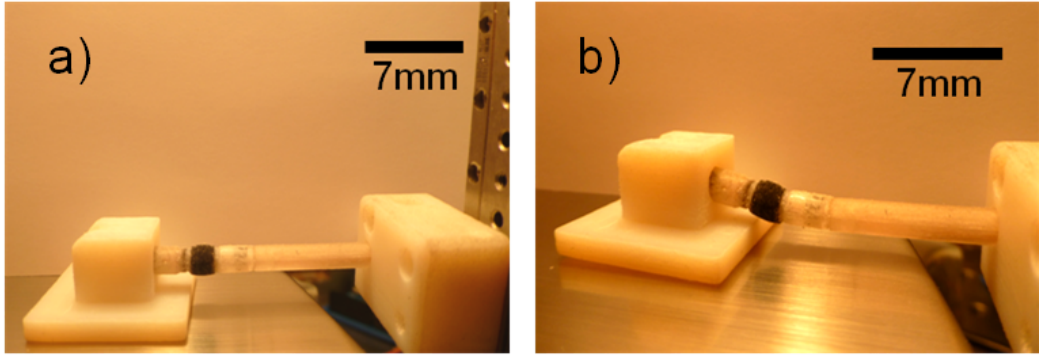


Figure 14: Lateral calibration test run: fully released (a) and fully squeezed (b).

The first observation can be explained with the membrane structure. The membrane is mainly designed to deal with axial forces. Its deflection response to lateral forces does not necessarily have to be linear. Subsequently, the magnetic field - force relation cannot fit the Biot-Savart law. The second observation may occur due to the magnetisation of the permanent magnet. The magnet is magnetised in axial direction and, therefore, favours the measurement of axial magnetic flux densities. Changes in lateral magnetic flux densities are much harder to detect.

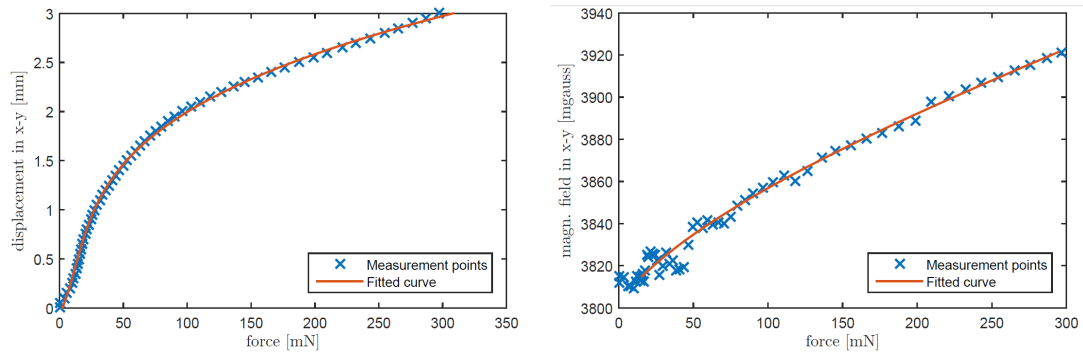


Figure 15: Lateral displacement - force behaviour (left) and magnetic field - force behaviour (right).

3.4 Catheter validation

In a second step, the calibrated catheter is validated within another test run as depicted in Figure 16.

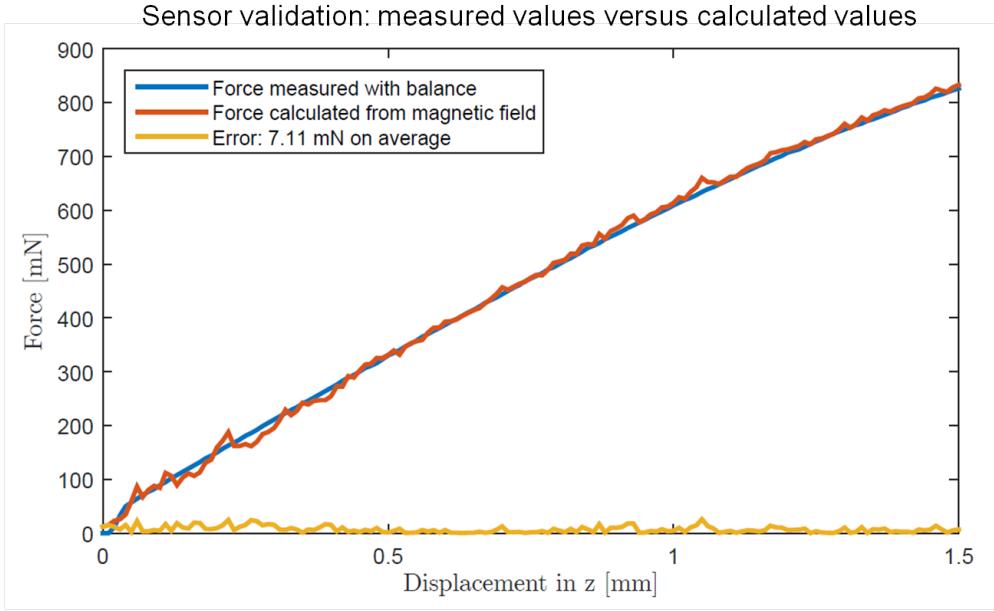


Figure 16: Catheter validation: measured force values versus calculated force values.

The applied contact force is calculated from the magnetic flux density data provided by the Hall sensor, using the relationship found during calibration (red curve). At the same time, the contact force is measured with a balance (blue curve). The respective error (green curve) is considerably small.

3.5 Material stiffness assessment

The intention of the material stiffness experiments is to prove the Force Sensing Catheter's ability to distinguish between hard and soft tissue. The calibrated catheter is used to push axially on three different material samples, namely steel, styrofoam and sponge (from stiff to soft). Additionally, the catheter is moved freely in ambient air for reference purpose (see Figure 17). Each of the samples is squeezed until 400 mN are reached. This is the equivalent of 40 g contact force and, thus, the double of the recommended contact force for cardiac ablations.

Stiff tissue leads to a faster deflection of the catheter membrane as shown in Figure 17. In air, the catheter displaces freely with no membrane compression at all. However, noise of external magnetic fields can be observed.

The noise in Figure 17 occurs due to locally changing external magnetic fields. The mitigation of such disturbance effects is discussed in Chapter 4.2.

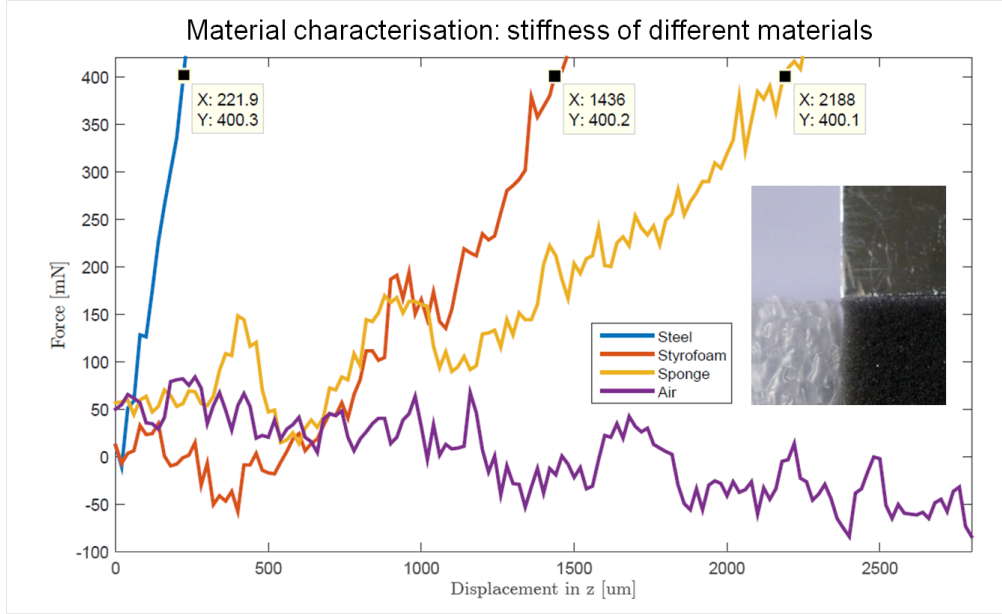


Figure 17: Assessment of different material stiffnesses: steeper force - displacement curves for stiffer materials.

3.6 Tissue diagnosis

Tissue sensing with the help of catheters might be used to categorise living tissue inside the human body. Healthy cells generally carry more water than dead cells do. Consequently, healthy cells show a softer behaviour once they are squeezed.



Figure 18: Force Sensing Catheter pushing muscle tissue.

The Force Sensing Catheter is used as a sensing device to execute tissue indentation. The catheter tip follows a pre-generated trajectory along the tissue

surface. At every measurement point, the catheter moves towards the tissue and pushes the tissue surface until a certain threshold force is reached. The required axial displacement indicates the flexibility of the tissue (cf. Chapter 3.5). Large displacements go along with soft tissue areas like fat whilst small displacements match with stiff tissue areas like bones.

The tissue diagnosis experiments are executed on a veal shank that is shown in Figure 18. Two piece of information can be mapped along the catheter trajectory. One of them is the surface of the tissue. A contact force will be sensed as soon as the catheter tip reaches the tissue surface. The associated catheter position is given by the micro-manipulator. The other one shows the tissue flexibility at every measurement point as shown in Figure 19 b). The flexibility is gained using the idea presented in Chapter 3.5.

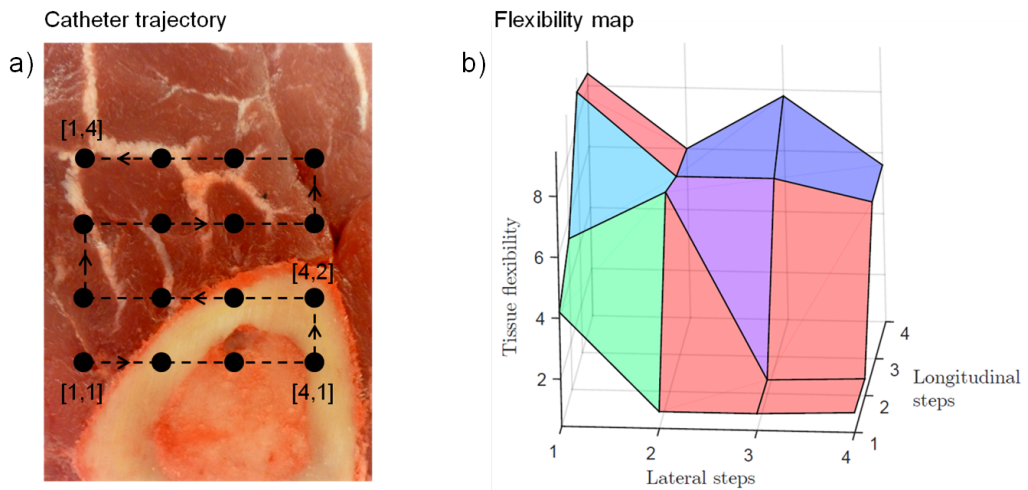


Figure 19: Tissue flexibility mapping.

Figure 19 illustrates a simple experiment for a short trajectory of 16 measurement points. However, the developed software is ready to automatically run extensive trajectories and map the respective flexibility along a tissue surface. The feasibility of large area tissue scans is currently limited by disturbances of external magnetic fields. Countermeasures are addressed in Chapter 4.2.

4 Conclusion

The following list summarises the achievements of this thesis regarding the development of a novel force sensing catheter:

- Smallest possible and flexible Hall sensor wiring solution.
- Flexible membrane design including simulations for the squeezing behaviour.
- 1D catheter design: cast silicon membrane with 1.6 mm outer diameter.
- 3D catheter design: printed plug connector model including stiff parts and a flexible membrane at 3.5 mm outer diameter.
- B-field simulations for theoretical insights on the Hall sensor behaviour with respect to its displacement from the magnet.
- Calibration and validation of the 3D catheter model.
- Tissue indentation with the 3D catheter.

In the following, the conclusion addresses limitations, optimisations, applications and advantages of the Force Sensing Catheter.

4.1 Limitations of the Force Sensing Catheter

The Force Sensing Catheter at its present state faces four principal limitations.

First of all, the measured B-field values are influenced by noise of external magnetic fields.

Secondly, the Force Sensing Catheter does not make use of the full measurement range of the Hall sensor. The full range would be +/- 16 Gauss[8] whereas the Force Sensing Catheter mainly operates between 8 and 12 Gauss.

Thirdly, the current manufacturing process on a 3D printer does not satisfy highest demands regarding precision, accuracy and durability of the catheter.

Finally, the Force Sensing Catheter is limited in size to a minimal outer diameter of at least 3 mm for the 3D model. This dimension constraint arises from the Hall sensor edge length that measures 2 mm.

4.2 Outlook for future improvements

Future improvements shall mainly attack the present limitations of the Force Sensing Catheter.

First, noise caused by external magnetic fields should be subtracted during data post-processing if it is known. Preferably, the catheter head including the permanent magnet and the Hall sensor shall be screened against external fields.

Second, the measurement range and the measurement resolution of the Force Sensing Catheter can be improved. Optimising the strength and the shape of the magnet in combination with its distance from the Hall sensor will do so. Most importantly, the measurement range should be moved to the area of the declining B-field curve where the gradient is steepest (see Figure 6). The measuring intervals of the magnetic flux density between two deflection points will be maximal in this area. Noise will become less significant as a side effect of an increased range.

Third, more sophisticated manufacturing processes and materials will lead to an enhanced catheter performance regarding precision, accuracy and durability.

Last, further reductions in catheter size might be possible if smaller Hall sensors become available. Another option worth investigating is the usage of a 1D Hall sensor for the measurement of axial and lateral forces. Simulations as well as experiments show that the axial magnetic flux density does not only change due to axial forces but also due to lateral forces. If the characteristics of the two changing behaviours are distinct enough, a 1D Hall sensor might serve for 3D contact force measurements. Therefore, a drastic reduction of the outer catheter diameter would become feasible.

In addition, a steerability and localisation concept involving OctoMag[5] should be elaborated. The usage of a second permanent magnet for navigation and localisation purpose might be a promising idea to start with.

4.3 Possible applications of the Force Sensing Catheter

The main and initial application of the Force Sensing Catheter remains the radio-frequency cardiac ablation for the medical treatment of arrhythmia. Two further user scenarios can be identified today. One of them is the usage of the small 1D catheter model for measurements of the human brain pressure. The other one is

the tissue diagnostics tool discussed in Chapter 3.6.

4.4 Advantages of the Force Sensing Catheter

The Force Sensing Catheter measures axial and lateral forces. It makes use of a simple force sensing principle that relies on a Hall sensor and a permanent magnet only. The Force Sensing Catheter comes with a small and compact design. The outer diameter of the 3D-printed prototype already matches the state of the art. Furthermore, the design of the Force Sensing Catheter includes the option for simple navigation and localisation of the catheter head using external magnetic fields.

References

- [1] Biosense Webster. Thermocool® SmartTouch® Catheter Resources. <http://www.biosensewebster.com/co-smarttouch.php>. Accessed January 16, 2015.
- [2] Biotronik SE & Co.KG. Katheterbehandlung zur Verödung störender Gewebeareale. http://www.biotronik.com/wps/wcm/connect/de_de_web/biotronik/sub_top/patients/Diseases_and_diagnoses_en/cardiac+arrhythmia/ablation/page_katheterablation_zur_Behandlung_von_vorhofarrhythmien. Accessed January 16, 2015.
- [3] E. P. Furlani. *Permanent Magnet and Electromechanical Devices*. Academic Press, 2001.
- [4] HKCM Engineering. Fachhandel für Magnete: Ringe, Rohre. <https://www.hkcm.de/expert.php?fav=>. Accessed January 17, 2015.
- [5] M. P. Kummer, J. J. Abbott, B. E. Kratochvil, R. Borer, A. Sengul, and B. J. Nelson. OctoMag: An electromagnetic system for 5-DOF wireless micromanipulation. *Robotics, IEEE Transactions on*, 26(6):1006–1017, 2010.
- [6] V. Y. Reddy, D. Shah, J. Kautzner, B. Schmidt, N. Saoudi, C. Herrera, P. Jaïs, G. Hindricks, P. Peichl, A. Yulzari, et al. The relationship between contact force and clinical outcome during radiofrequency catheter ablation of atrial fibrillation in the TOCCATA study. *Heart Rhythm*, 9(11):1789–1795, 2012.
- [7] St.Jude Medical. TactiCath™ Quartz Contact Force Ablation Catheter. <http://professional-intl.sjm.com/therapies/tacticath-quartz/home>. Accessed January 16, 2015.
- [8] STMicroelectronics. LIS3MDL. http://www.st.com/web/en/catalog/sense_power/FM89/SC1449/PF255198?s_searchtype=keyword. Accessed January 17, 2015.
- [9] StopAfib.org. Contact Force Sensing RF Catheters for Ablation. <http://www.stopafib.org/catheter-ablation/technology-contactforce.cfm>. Accessed January 16, 2015.

- [10] Stratasys. Objet500 Connex. <http://www.stratasys.com/3d-printers/design-series/connex-systems>. Accessed January 17, 2015.
- [11] A. Thiagalingam, A. DAVILA, L. Foley, J. Guerrero, H. Lambert, G. Leo, J. N. Ruskin, and V. Y. Reddy. Importance of Catheter Contact Force During Irrigated Radiofrequency Ablation: Evaluation in a Porcine Ex Vivo Model Using a Force-Sensing Catheter. *Journal of cardiovascular electrophysiology*, 21(7):806–811, 2010.
- [12] W. C. Young and R. G. Budynas. *Roark's Formulas for Stress and Strain*. McGraw-Hill, 7th Ed., 2012.

A Functional principle of a Hall sensor

A B-field exerts forces on electrical currents running through conductors. In a Hall sensor, the input current I is deflected from its original path by the B-field B . Therefore, a negative charge occurs on one side of the Hall sensor whereas the other side becomes charged positively. The potential difference is measured as the Hall voltage U .

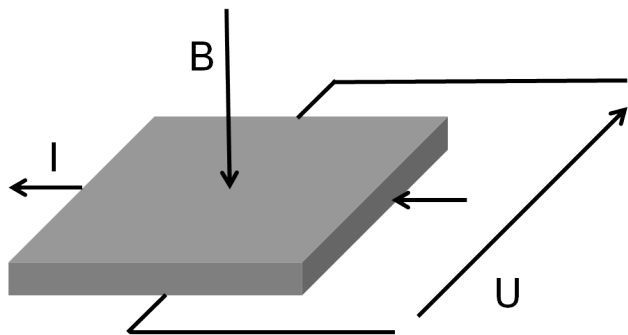


Figure 20: Functional principle of a Hall sensor.

B Simulations for the membrane deflection

This chapter discusses the simulations for the strategic development of a suitable membrane for the Force Sensing Catheter. A suitable membrane shows a desired deflection behaviour under an applied contact force. A desired deflection behaviour shall be in a range that allows the precise calculation of contact forces through the measurement data of the Hall sensor. The main design parameters to choose are the thickness and the material stiffness of the membrane.

In a first step, simulations for the membrane deflection behaviour are executed for a generic and simplified case. A radially fixed silicone disk is axially pushed with a small contact force as shown in Figure 21. Varying the disk parameters allows to gain a feeling for the deflection behaviour. The disk shown in Figure 21 has a diameter of 3 mm and a thickness of 0.5 mm. It is pushed with a contact force of 1 N.

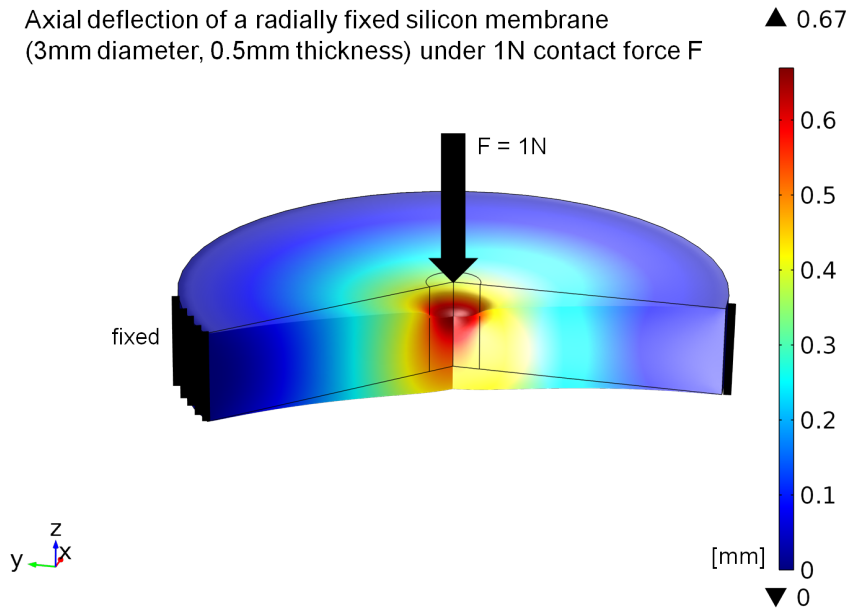


Figure 21: Deflection of a radially fixed silicon disk under a contact force.

The deflection response for a range of contact forces for three different membrane thicknesses is illustrated in Figure 22. The maximal overall deflection of the membrane in Figure 21 (around 0.4 on the scale) corresponds to the value of the red curve in Figure 22 at 1000 mN applied force.

Two basic insights are gained from the simulation shown in Figure 22. Firstly,

the membrane deflection scales linearly with the applied contact force. Secondly, the thinner the membrane the more it deflects for the same contact force.

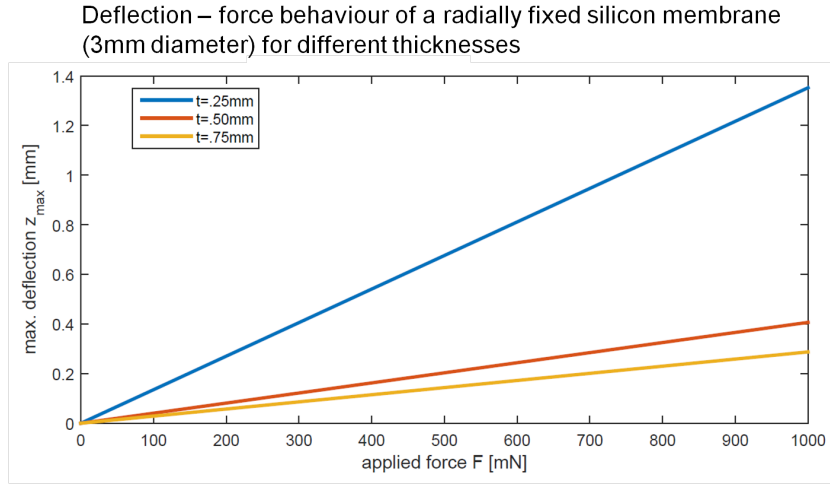


Figure 22: Membrane deflections in dependency of the applied force for different thicknesses.

In a next step, the simulations for the simplified case of a radially fixed silicone disk are validated with hand calculations. The hand calculations are based on the theory of "Roark's Formulas for Stress and Strain" [12], p.492, case 17. The simulations match with the analytical expectations (cf. Figure 23). One further insight is revealed in Figure 23: The membrane deflection decays with the third potency of its thickness.

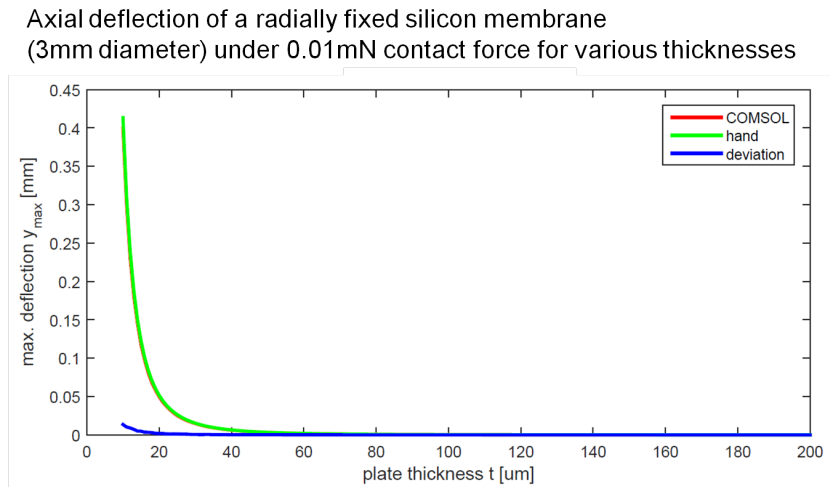


Figure 23: Membrane deflection: hand validation of the COMSOL simulations.

Summing up all the observations gained through simulations enables the tailor-made design of deflection membranes. Further, the designs can be validated and its parameters optimised through approved simulations with real geometries.

Thus, in a final step, the simulation model is applied to real geometries of catheter membranes. Figure 24 shows a possible membrane of a 1D Force Sensing Catheter and its axial deflection response to a contact force of 1 N. The hollow silicon membrane depicted in Figure 24 is 3.5 mm high, has an outer diameter of 2 mm, an inner diameter of 1 mm and, thus, a wall thickness of 0.5 mm.

**Axial deflection of a hollow silicon membrane
(2mm outer diameter, 1mm inner diameter, 0.5mm wall thickness,
3.5 mm height) under 1N contact force F**

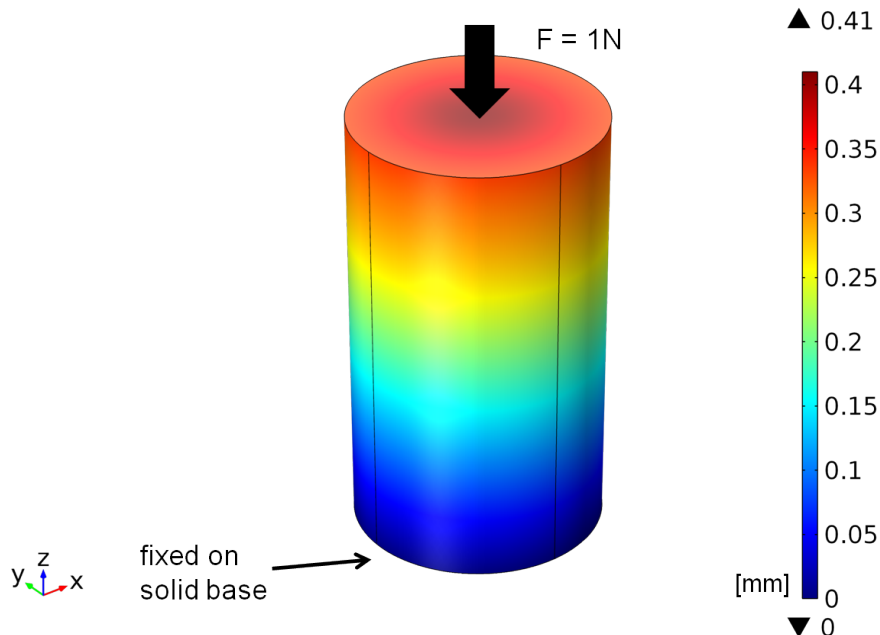


Figure 24: Membrane deflection of the 1D Force Sensing Catheter.

C Code for the experiments

This chapter presents code fragments for the generation of trajectories and for the evaluation and post-processing of the measurement data. The complete code files can be found on the data disc of the Force Sensing Catheter thesis.

The LabView code for the operation of the micro-manipulator and the logging of the experimental data was developed by Simone Gervasoni.

C.1 Trajectory generation

This section shows a possible MATLAB code for a forth-and-back tissue sensing trajectory. A matrix is filled with desired measurement points according to the tissue dimensions. The matrix is exported as a .txt-file. Subsequently, the .txt-file is fed into LabView. LabView finally operates the micro-manipulator. The micro-manipulator moves the catheter.

Simpler trajectories like the one for axial calibration can just as well be written directly by hand into a .txt-file.

```
% _____
% FORCE SENSING CATHETER
% Trajectory generation for tissue sensing
% 16/01/15
% Florian Berlinger
% _____
```



```
%% INITIALISE TISSUE
l = 100; % steakwidth [mm]
w = 100; % steakwidth [mm]
p = 2; % push range in z-direction [mm]
step = 10; % distance btw. measurement points [mm]
```



```
%% GENERATE AWESOME TRAJECTORY
```

```

x = zeros(); y = zeros(); z = zeros();

for i = 0 : l/step
    x(((w/step+1)*i+1)*12+1):(((w/step+1)*i+(w/step
        +1)*12+12)) ...
    = i * step;

s = (-1)^i; % sign for y-direction [-]
r = rem(i,2); % remainder after division of i by
2, either 0 or 1 [-]

for j = 0 : w/step
    y(((j+1 + i*(w/step+1))*12+1):((j+1 + i
        *(w/step+1))*12+12)) ...
    = s * j * step + r * w;

    for k = 0 : 10
        z(k+1) = k * p/10;
    z(12) = 0;

    end
end
end

% Repeat z-deflection at every measurement point
z = z';
z = repmat(z, (l/step+1) * (w/step+1), 1);

% Cut the crap
x = x(13:end);
y = y(13:end);

```

```

%% CHECK TRAJECTORY AND EXPORT DATA POINTS
% Trajectory visualisation
plot3(x, y, -z, 'LineWidth', 1)
xlabel('x-direction')
ylabel('y-direction')
zlabel('z-deflection')
axis([min(x)-5 max(x)+5 min(y)-5 max(y)+5 -p-.1 0+.1])

% Convert millimeters to meters for SmarAct
x = x*1e-3;
y = y*1e-3;
z = z*1e-3;

% Write trajectory
tra = [x' y' -z']; % open tra in workspace and copy the
values to a .txt-file

```

C.2 Data post-processing

This section shows a possible MATLAB code for data post-processing. The gained measurement datasets are averaged over several experiment. Measurement outliers are filtered. A curve fitting is done to find the polynomial equation between the measured magnetic flux densitiy and the measured contact force. The testing results are visualised in several plots.

```

% -----
% FORCE SENSING CATHETER
% Sensor calibration
% 08/01/15
% Florian Berlinger
%
```

```

%% LOAD EXPERIMENTAL DATA

```

```

data1 = load( 'exp080115_15_-1500.txt' );
data2 = load( 'exp080115_17_-1500.txt' );
data3 = load( 'exp080115_18_-1500.txt' );
data4 = load( 'exp080115_19_-1500.txt' );
data5 = load( 'exp080115_20_-1500.txt' );
data6 = load( 'exp080115_21_-1500.txt' );

%% DATA POST-PROCESSING
% Displacement vector [mm]
D = [ data1(:,2) data2(:,2) data4(:,2) data5(:,2) data6
      (:,2) ]*1e3;
d = abs(D);
d = mean(d');

% Mean force vector [mN]
F = [ data1(:,4) data2(:,4) data4(:,4) data5(:,4) data6
      (:,4) ]*10;
f = mean(F');

% Mean magnetic field vector [mgauss]
M = [ data1(:,6) data2(:,6) data4(:,6) data5(:,6) data6
      (:,6) ];
m = mean(M');

% Outrageously sexy outlier filter
avgstep = (m(end)-m(1))/(length(m)-1);
% average step width (1st & last
% measurement must be true!)

n = 0;
% outlier counter
for i = 1:length(m')-1

```

```

if abs(m( i+1)-m( i )) > 5*avgstep           % step very
unlike average step
    m( i+1) = m( i ) + avgstep;           % overwrite value
with average value
    n = n+1;
end
end

fprintf('%'g_outliers_overwritten_during_post-processing.\n
', n)
fprintf('\'n')

%% CURVE FITTING
% Force from deflection (F=k*d)
eq_k = polyfit(d, f, 1);

fprintf('The_force-deflection_relation_is:f=%g*d+%g,\n
n', eq_k(1), eq_k(2))
fprintf('where_d_is_the_given_deflection_and_f_is_the_
requested_force.\'n')
fprintf('Therefore, the_membrane_stiffness_is:k=%g.\'n',
eq_k(1))
fprintf('\'n')

d2_k = d(1):1:d(end);
f2_k = polyval(eq_k, d2_k);

% Force from magnetic field
eq_m = polyfit(m, f, 3);

fprintf('The_force-magnetic_field_relation_is:f=%g*m^3 +
%g*m^2+%g*m+%g,\'n', eq_m(1), eq_m(2), eq_m(3),
eq_m(4))

```

```
fprintf( 'where m is the measured magnetic field and f is the requested force.\n' )

m2_m = m(1):1:m(end);
f2_m = polyval(eq_m, m2_m);

%% FIGURES
% Mean force plot
fig1 = figure(1);
set(fig1, 'OuterPosition', pos1);
plot(f, '*')
hold on
plot(data1(:,4)*10)
hold on
plot(data2(:,4)*10)
hold on
plot(data4(:,4)*10)
hold on
plot(data5(:,4)*10)
hold on
plot(data6(:,4)*10)
title('Mean force')

% Mean magnetic field plot
fig2 = figure(2);
set(fig2, 'OuterPosition', pos2);
plot(m, '*')
hold on
plot(data1(:,6))
hold on
plot(data2(:,6))
hold on
plot(data4(:,6))
```

```
hold on
plot(data5(:,6))
hold on
plot(data6(:,6))
title('Mean_magnetic_field')

% Displacement versus force plot
fig3 = figure(3);
set(fig3, 'OuterPosition', pos3);
plot(f, d, 'o', f2_k, d2_k, 'Linewidth', 3)
title('Displacement_verseus_force')
xlabel('force_[mN]')
ylabel('displacement_in_z_[mm]')

% Magnetic field versus force plot with fitted curve
fig4 = figure(4);
set(fig4, 'OuterPosition', pos4);
plot(f, m, 'o', f2_m, m2_m, 'Linewidth', 3)
title('Magnetic_field_verseus_force')
xlabel('force_[mN]')
ylabel('magn._field_in_z_[mgauss]')
legend('Post-processed_measurement_points', 'Fitted_curve',
       'Location', 'SouthEast')
```

